Original articles

The synergy of transformation of isomorphous phyllosilicate structures

A. G. Chetverikova[1]✉, V. N. Makarov[1], O. N. Kanygina[1], M. M. Seregin[2], A. A. Yudin[1]

*[1]Orenburg State University,
13 Pobedy ave., Orenburg 460018, Russian Federation*

*[2]LLC «BO-ENERGO.ASTS»,
19 Prospect Mira, building 1, Moscow 129090, Russian Federation*

Abstract

The article presents an analysis of the synergy of structural transformations of phyllosilicates subjected to high temperatures and microwave radiation in terms of the destruction and formation of crystal structures. Studying the synergy of transformations of crystal structures is essential for the development of new materials and technologies, because it helps to create materials with unique properties, which cannot be obtained when using the same factors separately.

The material used in the study was a polymineral complex, which contained quartz, montmorillonite, kaolinite, chlorite, paragonite, and iron oxides (listed from the largest to the smallest mass fraction). The methods used in the study allowed us to assess the structural transformations. Averaged structural formulas of the studied phyllosilicates were calculated using the oxygen method combined with a recalculation method based on the results of a microprobe analysis. Differential thermal analysis demonstrated a synergistic effect of high temperature and microwave fields registered as a decrease in the temperature gradient of the ceramics and initiation of the sintering process at lower temperatures and with greater intensity. All the treated samples contained the amorphous phase in significant concentrations: from 15 to 25 vol. %. Half of the three-layer phyllosilicates (chlorite and montmorillonite) were destroyed by the microwave field. Kaolinite and paragonite practically did not react to external factors. The synergistic effect was the most obvious in the structural transformations of silicon and iron oxides.

Our experiments demonstrated for the first time the mechanism of formation of magnetite and hematite crystals from X-ray amorphous iron-containing films covering the particles of clay minerals. The use of the MW field and the resulting dehydration led to the formation of crystals of nuclei of iron oxides. The following high-temperature processes activated an increase in aggregated iron (magnetite and hematite). The X-ray diffraction analysis determined the presence of a synergistic effect in the evolution of structures, which could not be identified by means of IR-spectroscopy. The EPR spectroscopy allowed us to register the states of rare irregular cells with foreign paramagnetic atoms. The shift of the foreign Fe^{3+} from the geometric centers of octahedral crystal cells towards the minima of potential energy caused by the Jahn-Teller effect decreased the potential energy of the crystal lattice. At the same time, some chemical bonds forming the crystal cell became stronger, while others weakened.

Keywords: Crystal cell, Transformation, Montmorillonite, Kaolinite, Chlorite, Paragonite, Microwave field, Heat treatment

✉ Anna G. Chetverikova, e-mail: kr-727@mail.ru

Condensed Matter and Interphases / Конденсированные среды и межфазные границы   2024;26(2): 327–338

A. G. Chetverikova et al.   The synergy of transformation of isomorphous phyllosilicate structures

1. Introduction

Within the modern paradigm, a structure has the following characteristics: morphometric (size, shape, surface of the structural elements, and their quantitative description), geometric (spatial composition of the structural elements), and energy characteristics (types of structural bonds and the total energy of the structure). However, this approach does not fully reflect the dynamics of structures that have spatial and temporal nature [1].

The synergy of transformation of a crystal structure is a combination of processes facilitating its evolution at various levels. Interactions can occur between physical parameters, for instance temperature and electromagnetic fields, and between chemical factors, including the concentration of foreign ions or phases and synthesis activators [2, 3].

Studying the synergy of transformations of crystal structures is essential for the development of new materials and technologies, because it helps to create materials with unique properties, which cannot be obtained when using the same factors separately. The synergistic effect results in the formation of new crystal phases, which have higher thermal conductivity and strength [4] or flame retardancy [5]. There are some studies focusing on the combined effect of the temperature field, the microwave field, and impurity ions on condensed matter [6]. However, there appear to be no publications concerning the synergistic effect of these factors during the transformation of crystal cells of phyllosilicates.

Earlier studies demonstrated that microwave field treatment of montmorillonite can result in structural transformations (restructuring of the crystal structure and amorphization) caused by heating [7]. It is known [8, 9] that high temperature treatment of phyllosilicates results in the structural degradation of clay minerals.

In order to develop functional materials with good sorption properties, it is important to analyze the effect of various fields on phyllosilicates. [10] considers the effect of a 10-minute exposure to microwave radiation on the morphology, phase composition, and sorption capacity of montmorillonite clay. The authors demonstrated that phyllosilicates can be modified, but did not explain the transformations occurring at micro- and mesolevels. [11] determined that both resistance heating and microwave radiation have a positive effect on the sorption capacity of montmorillonite. The authors suggested a hypothesis that the changes in the sorption properties of phyllosilicate containing materials subjected to MW field and heat treatment are caused by the transformation of isomorphous structures.

It is therefore important to consider the synergistic effect of high temperature and microwave radiation on structural transformation of the particles of the montmorillonite polymineral complex (M-PMC).

The purpose of our study was to analyze the synergy of structural transformations of phyllosilicates subjected to high temperatures and microwave radiation in terms of destruction and formation of crystal structures.

2. Experimental

2.1. Materials

In our study, we analyzed samples of montmorillonite clay (M-PMC) mined in the Orenburg Region. The samples were ground using an iMold milling machine and subjected to sieve analysis with the mesh size of 26 µm. The montmorillonite yield of the polymineral complex was over 30% and the total amount of clay minerals was – 50%. A large number of organic compounds determined by means of Raman spectroscopy were removed with a 30% H_2O_2 solution.

The elemental composition of the obtained A sample, expressed in form of oxides, was determined by means of chemical analysis according to [12]. According to the X-ray powder diffraction performed in [13] clay is a polymineral complex, which contains quartz, montmorillonite, kaolinite, chlorite, paragonite, and iron oxides (listed from the largest to the smallest mass fraction). Table 1 presents the structural formulas and volume fractions of their crystalline phases in the A sample.

Powder samples (**A**) were subjected to microwave radiation for 10 minutes. The source of the MW field was a 750 W magnetron with a radiation frequency of 2.45 GHz [14]. A 10 mm layer of dispersed samples was put into a

Condensed Matter and Interphases / Конденсированные среды и межфазные границы   2024;26(2): 327–338

A. G. Chetverikova et al.   The synergy of transformation of isomorphous phyllosilicate structures

cuvette on a rotating plate in order to average the heating conditions at a humidity of 70±5% (sample **B)**. The temperature of the samples in the MW field was up to 220–250 °C. The third sample **C** was heated to 900 °C at a heating rate of 5 °C/min. The fourth sample **BC** was obtained by sequential MW irradiation and heating up to 900 °C.

The understanding and modeling of structural transformations caused by the synergistic effect of the MW field and high temperatures requires a comprehensive experimental analysis at millimeter-, micro-, and nanosize levels. Accurate information can only be obtained when controlling the reproducibility of results. In our study, we used methods that allowed us to assess the dynamics of structural transformations caused by MW field and temperature in the presence of foreign elements. In particular, we focused on crystallochemical characteristics (2.1), physicochemical properties (2.2–2.5), and the fine structure (method 2.6).

2.2. Crystallochemical analysis

Structural formulas given in Table 1 do not show the distribution of the foreign elements between tetrahedral, octahedral, and interlayer positions in the crystal lattice. According to [15], these positions should be taken into account when analyzing the chemical structure of layered silicates. In order to calculate the crystal chemical formulas of the studied phyllosilicates, we used a classical oxygen method combined with a recalculation method based on the results of a microprobe analysis [16].

2.3. Differential thermal analysis

Structural transformations in the samples were registered by means of differential thermal analysis (DTA). The thermograms were obtained using a Thermoscan-2 unit (OOO Analitpribor, Russia) with a heating rate of 5 °C/min from 25 to 1000 °C. The error for temperature measurement was ± 1 °C. Aluminum oxide powder (Al_2O_3) with a weight of 0.5 g and sealed in a quartz container was used as a reference. The weight of the studied sample put into a quartz crucible was 0.50±0.01 g.

2.4. Infrared spectroscopy

The IR spectra of the samples were obtained using an Infralyum FT-02 IR Fourier spectrometer (OOO Lumex, Russia). The spectrometer had an attachment for disturbed total internal reflection (DTIR) with a single reflection zinc selenide (ZnSe) crystal. The measurements were performed over the range of $550 \div 4000$ cm^{-1} with a resolution of 2 cm^{-1}. The Bessel apodization was used for the Fourier transform. The spectra were recorded in the mode of accumulation of 60 scans with the correction of the base line.

2.5. X-ray phase analysis

The X-ray phase analysis of the powders was conducted using a Shimadzu XRD 7000S diffractometer (Shimadzu Corporation, Japan) with a OneSight matrix detector. Diffraction patterns were recorded under the following

Table 1. Phase composition of the sample

Mineral / Space group [12]	Structural formula / mineral classification [13]	Fraction, vol. %
β-Quartz $P6_222$	SiO_2 Simple oxide	>40
Montmorillonite $B2/m$	$(Na,Ca)_{0.33}(Al_{1.67}Mg_{0.33})(Si_4O_{10})(OH)_2 \cdot nH_2O$ three-layer phyllosilicate (T-O-T): two tetrahedral silica-oxygen (T) and one octahedral alumina-oxygen (O) sheets	30
Kaolinite $P1$	$Al_2(Si_2O_5)(OH)_4$ two-layer phyllosilicate: T-O structure	10
Chlorite $C2/m$	$(Mg,Fe)_{6-x}(Al,Fe)_{2x}Si_{4-x}O_{10}(OH)_8$ three-layer phyllosilicate: T-O-T structure	10
Paragonite $B2/b$	$NaAl_2(Si_3Al)O_{10}(OH)_2$ two-layer phyllosilicate: T-O structure	5
Magnetite, hematite $Fd\bar{3}m, R\bar{3}$	$Fe^{2+}Fe^{3+}_2O_4, Fe_2O_3$ Simple oxide	<5

Condensed Matter and Interphases / Конденсированные среды и межфазные границы   2024;26(2): 327–338

A. G. Chetverikova et al.   The synergy of transformation of isomorphous phyllosilicate structures

conditions: anode of the X-ray tube – Cu (copper), rotation of the sample, angles 2θ: from 5 to 140°, scanning rate of 1 °/min, step of 0.2°.

2.6 EPR spectroscopy

The EPR spectra of the initial samples and the treated samples were registered using a CMS8400 compact automatic controlled spectrometer (Adani, Belarus) at room temperature. The spectra were registered under the following conditions: frequency of 9.86 GHz, magnetic field of 1–7 T, magnetic field modulation frequency of 200 kHz.

## 3. Results and discussion

3.1. Structural formulas of phyllosilicates with isomorphous ions

Morphometric and monomineral analyses of the M-PMC samples were performed using a JCM-6000 scanning electron microscope (JEOL, Japan). Fig. 1a demonstrates the matrix structure of the dispersion system: the microstructure consists of solid structural elements (Fig. 1b), i.e. mineral particles, oxide grains, and their associations that determine the dispersion of the system. It is obvious that the structure consists of powdered quartz grains (1) and microaggregates of clay (2) and clay powder particles (3). The powdered grains were rounded and had the elemental composition of Si, O; their size varied from 1 to 5 μm. Some of the quartz grains were, as usual [17], covered with a thin film of iron oxides, and some were covered with clay coats. Microaggregates (2) consisted of clay particles
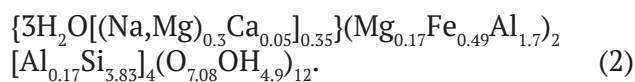
of kaolinite (O, Si, Al, Fe, Ti), mostly isometric or slightly elongated and with the size varying from fractions of a micron to several microns.

Isometric microaggregates (3) were looser and consisted of fine thin particles connected by clay bridges. Their size was 10–20 μm. Montmorillonite and chlorite microaggregates with similar crystal structures and microelemental composition (O, Si, Al, Fe, Na, Mg, Ca) usually have a thin leaf-like shape [18]. The boundaries between the primary particles were hardly identifiable because one microaggregate gradually transformed into another.

A general crystal chemical formula of montmorillonite taking into account the isomorphous ions is presented as follows [19]:

$$M_x^+Si_4Al_{2-x}(Fe^{2+}, Mg)_xO_{10}(OH)_2 \cdot nH_2O. \qquad (1)$$
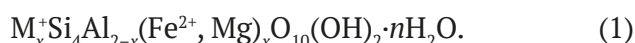
x varies within quite a wide range (from 0.1 to 0.6), because it is often impossible to obtain a monomineral fraction of the clay mineral for chemical analysis. Metal cations (M) are represented by ions of alkali and alkaline earth elements (Na, Ca, Mg, etc.) located in the interlayers of the structure. They compensate for the negative charge of the octahedral layers. The calculated formula of the studied montmorillonite is presented as follows (2):

$$\{3H_2O[(Na,Mg)_{0.3}Ca_{0.05}]_{0.35}\}(Mg_{0.17}Fe_{0.49}Al_{1.7})_2$$
$$[Al_{0.17}Si_{3.83}]_4(O_{7.08}OH_{4.9})_{12}. \qquad (2)$$

The averaged calculated structural formula of kaolinite also demonstrates a high degree of isomorphism:
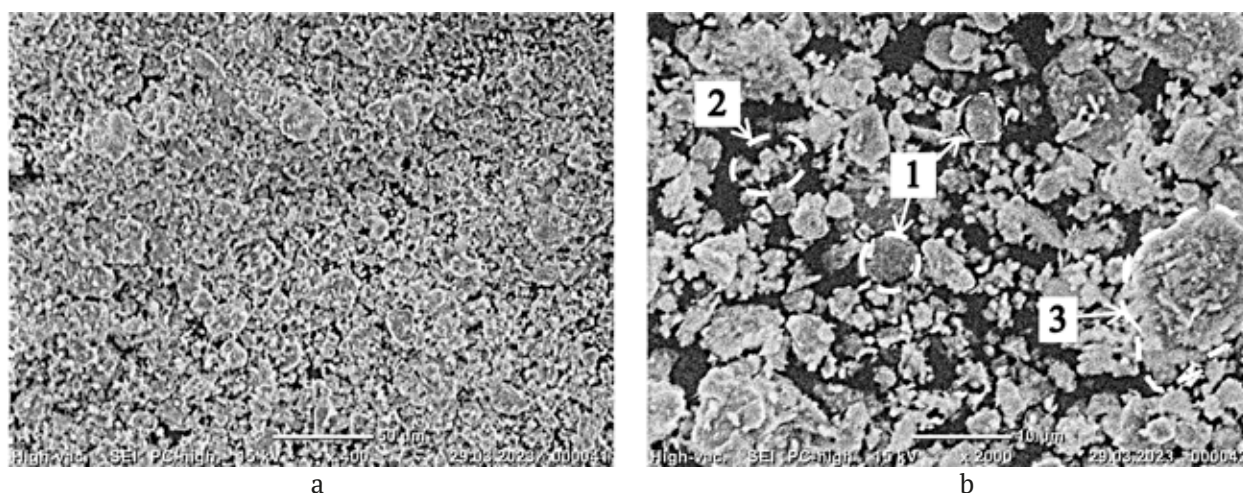
Fig. 1. Matrix microstructure: general view (a) and solid structural elements (b)

Condensed Matter and Interphases / Конденсированные среды и межфазные границы   2024;26(2): 327–338

A. G. Chetverikova et al.   The synergy of transformation of isomorphous phyllosilicate structures

$$Na_{0.12}Ca_{0.02}(Mg_{0.12}Fe_{0.27}Al_{3.59})[Al_{0.41}Si_{3.59}O_{10}]\cdot(OH)_8. \quad (3)$$
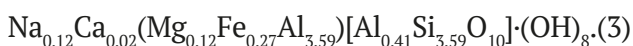
Chlorite should have a strictly specific structure without any deviations in the ratios of group coefficients. Therefore, the recalculated structural formula (4) is close to a typical chlorite formula:

$$(Mg_{0.51}Ca_{1.2}Fe_{1.19}Al_{3.07})_{5.97}(Si_{3.12}Al_{0.88})_4O_{10}(OH)_8. \quad (4)$$
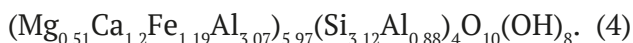
The structural formula of paragonite cannot be specified due to its low concentration (because it is difficult to obtain a monomineralic fraction).

3.2. Interpretation of the differential thermal analysis (DTA)

Fig. 2 presents the thermograms of samples **A** and B. Analyzing the empirical dependences, we identified 5 main stages of structural transformation of the A and B samples. The obtained thermograms of A and B are in good agreement with the results obtained in [20].

During the first stage of heating (from 25 to 310 ºC) of the A sample, an intense endothermic effect was observed, which is quite common for complexes containing clay minerals. During this stage, most of the water is removed from interparticle capillaries and the diffuse region of the electrical double layer [21]. The derivatogram of the B sample did not demonstrate any endothermic effects during this stage. Most of the physically bound water was removed as a result of the MW radiation.

During the second stage, the condition of the A and B samples stabilized, and all the energy was used for heating.
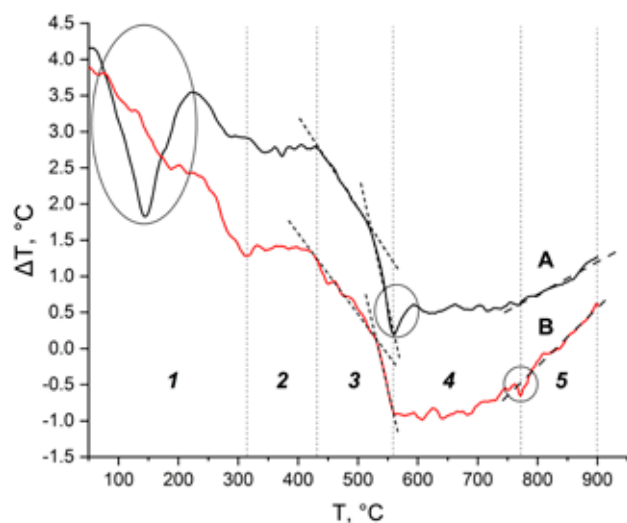
During the third stage, within the temperature range from 430 to 540 ºC, samples A and B demonstrated synchronized decomposition, which might be caused by the removal of chemically bound water from the structure of phyllosilicates [22, 23]. At the end of the third stage, another, less intense, endothermic effect was observed in the A sample. As a result, the dispersion system transformed into a more equilibrium state during the fourth stage. The effect is common for both metakaolinization of clay minerals within the set temperature range and the β→α-quartz transformation. There was not such an endothermic effect in the B sample.

During the fourth stage, at a temperature of about 700 ºC the sintering process (agglomeration) was observed in the B sample. The process started 70 ºC earlier and was more active than in the A sample. The sintering proceeded during the fifth stage. This is the synergistic effect of high temperature and the microwave field: their combined use resulted in a decrease in the temperature gradient of the **B** sample and facilitated the initiation of the sintering process at lower temperatures and with greater intensity.

3.3. Interpretation of the IR spectra (transformation of the chemical bonds)

The main task of the IR spectroscopy was to specify the nature of the chemical bonds in sample **A** and their transformations in samples **B**, **C**, and **BC**. The obtained IR spectra are presented
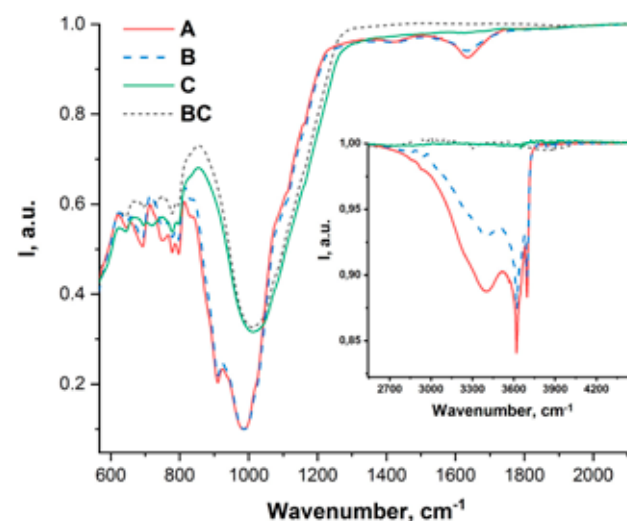

Fig. 2. Thermograms of samples **A** and **B**

Fig. 3. IR spectra of the samples: **A, B, C, BC**

Condensed Matter and Interphases / Конденсированные среды и межфазные границы   2024;26(2): 327–338

A. G. Chetverikova et al.   The synergy of transformation of isomorphous phyllosilicate structures

Table 2. Characteristic modes of interatomic bonds in M-PMC samples according to FTIR-spectroscopy results

Wavenumber, cm^{-1}				Oscillation type	Mineral
A	B	C	BC		
645	645	645	645	O-Si(Al)-O [24–26]	Montmorillonite/Chlorite, Kaolinite
693	693	694	694	Si-O [27]	Quartz
750	750	750	750	Si-O-Al [25, 26]	Kaolinite
778	778	778	778	Si-O [27]	Quartz
797	797	796	796		
833	833	831	831	Al(Mg)-OH [24–26, 28]	Montmorillonite, Kaolinite
878	878	–	–	Al(Fe)-OH [28]	Montmorillonite
911	910	–	–	Al(Al)-OH [25, 26, 28]	Montmorillonite, Kaolinite
935	935	–	–		
985	988	1010	1010	O-Si-O [24–26, 28]	Montmorillonite/Chlorite, Kaolinite
1025, 1113, 1164	1025, 1113, 1164	1088, 1164	1088, 1164		
1636	1636	–	–	Constitutional water (OH-group) [24, 28]	Montmorillonite/Chlorite
3397	3397	–	–		
3620	–	–	–	Constitutional water (OH-group) [25–27]	Kaolinite
3649, 3670, 3696	3620, 3649, 3670, 3696	–	–	Constitutional water (OH-group) [24–26, 28]	Montmorillonite, Kaolinite

in Fig. 3. The results of the analysis of the IR spectra are given in Table 2. The base lines of the spectra were corrected and the absorption maxima were normalized so that the samples with close structure of the absorption bands were as similar as possible.

When comparing the absorption bands of the obtained spectra to the results of previous studies it is impossible to reliably differentiate between montmorillonite and chlorite, when both of them are present in the clay, due to the similarity of their spectra [24].

A broad absorption band at 990–1000 cm^{-1} is explained by Si-O-Si vibrations in tetrahedral layers of montmorillonite or chlorite crystals [24, 28]. The presence of these minerals is confirmed by a profile near 3000–3700 cm^{-1}, where the **A**

spectrum shows a weak absorption band with a maximum at 3620 cm^{-1} caused by the vibrations of the O-H group in the three-layer structure of the mineral. Montmorillonite and chlorite have interlayer water molecules, which was demonstrated by an additional broad absorption band resulting from the O-H vibrations of the adsorbed water with the transmission minima at 3400 and 1636 cm^{-1} [24, 28]. Two clear intense peaks of the O-H vibrations at 3620 and 3696 cm^{-1} in the spectrum of the sample indicated the presence of kaolinite [25, 26]. Three absorption bands at – 1025, 1113, and 1164 cm^{-1} corresponded to the O-Si-O bonds in the kaolinite structure similar to the lines at 935 and 909 cm^{-1}, which appeared as a result of Al(Al)-OH vibrations.

Condensed Matter and Interphases / Конденсированные среды и межфазные границы   2024;26(2): 327–338

A. G. Chetverikova et al.   The synergy of transformation of isomorphous phyllosilicate structures

The intensity of the peak at 645 cm^{-1} corresponding to the bending vibrations of O-Si(Al)-O in chlorite was close to that of kaolinite bands [24].

For the main peak of the O-Si-O vibration, the montmorillonite lattice demonstrated adjacent lines corresponding to the bending vibrations of the O-H groups coordinated with Al(Al), Al(Mg), and Al(Fe). The presence of the absorption bands corresponding to the latter two substitutions indicated a significant level of isomorphism of the structures [24]. The studied M-PMC demonstrated intense Al(Mg)-OH absorption bands at 830 cm^{-1} and Al-(Fe)-OH - absorption bands at 878 cm^{-1}. Therefore, the A sample contained a large amount of magnesium and iron, which replaced aluminum in phyllosilicates crystals with the T-O-T structure.

A weak band at 694 cm^{-1} and even weaker bands at 777 and 796 cm^{-1} indicated the presence of quartz [27].

The spectra of the **B** samples demonstrated a decrease in the intensity of the absorption bands at 3386 and 1636 cm^{-1}, associated with the release of water molecules from the interlayer space of montmorillonite and chlorite.

The spectra of the **C** sample did not demonstrate any absorption bands corresponding to the vibrations of the OH groups. Besides, there were no broad absorption bands at 3380 and 1636 cm^{-1}, which indicated the absence of constitutional water in the structure. The identification of the obtained spectra was hindered by the possibility of formation of amorphous silicon oxide whose absorption bands overlapped with the absorption bands of anhydrous aluminosilicates.

The spectrum of the **BC** sample had the same absorption profile as the spectrum of the **C** sample. However, the relative intensities of both the main absorption band of the O-Si-O bond and the absorption bands at other wave numbers differed. We assume that this can be caused by the formation of various phases of the IR amorphous quartz and distorted structures of clay minerals.

We did not manage to determine the behavior of paragonite under various conditions by means of the IR spectroscopy, because the main absorption bands of this mineral overlapped with the absorption bands of the main phases of the M-PMC [29].
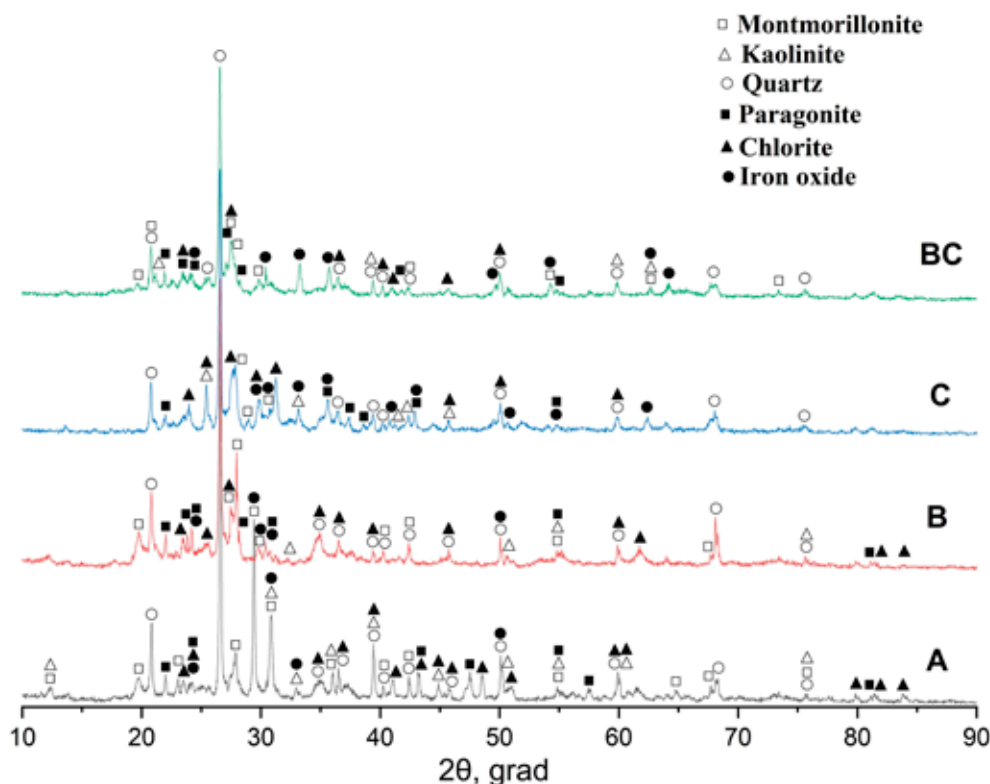

Fig. 4. Diffraction patterns of the samples: **A, B, C, BC** (bottom-up)

Condensed Matter and Interphases / Конденсированные среды и межфазные границы   2024;26(2): 327–338

A. G. Chetverikova et al.   The synergy of transformation of isomorphous phyllosilicate structures

3.4. Evolution of phase compositions

Fig. 4 shows the diffraction patterns of samples **A**, **B**, **C**, and **BC** (in the bottom-up order). The greatest effect observed for all the treated samples (B, C, BC) was the formation of an amorphous phase in significant concentrations. The most intense amorphization was registered for samples B (22 vol. %) and BC (25 vol. %). As a result of resistance heating up to 900 °C, 15% of crystalline modifications transformed into the amorphous phase.

The second greatest effect was the decomposition of 23% of montmorillonite. The main cause of this process was high-temperature heating (samples B and BC). Half of the montmorillonite crystal lattices were destroyed by the MW field (15%). Earlier we demonstrated [30] that the degree of amorphization of montmorillonite depends on the mode of the MW treatment and can reach up to 50–70%.

The next phyllosilicates whose crystal lattice was destroyed by the MW field was a thermally stable three-layer chlorite. Its volume fraction remained intact after heating (sample C), but was twice as small in samples B and BC.

Kaolinite and paragonite practically do not react to external factors: the distorted kaolinite cells disappear and paragonite crystallizes [31].

The synergistic effect was the most obvious in the structural transformations of silicon and iron oxides. Silicon oxides demonstrated a decrease in the symmetry of the newly formed phases and an increase in their specific surface as well as inhomogeneity of size distribution [32]. The fraction of quartz in samples **B** and **C** decreased by 5–7 %, while in the **BC** sample it decreased by 10–12 %. Our experiments demonstrated for the first time the mechanism of formation of magnetite and hematite crystals from X-ray amorphous (Table 1) iron containing films covering the particles of clay minerals (Fig. 1b). The use of the MW field and the resulting dehydration led to the formation of crystalline nuclei of iron oxides (sample **B**). At high temperatures, the formation of aggregated iron crystals (magnetite and hematite) intensified reaching the maximum level (11%) in sample **BC**.

The X-ray diffraction analysis determined the presence of a synergistic effect in the evolution of structures, which could not be identified by means of IR-spectroscopy.
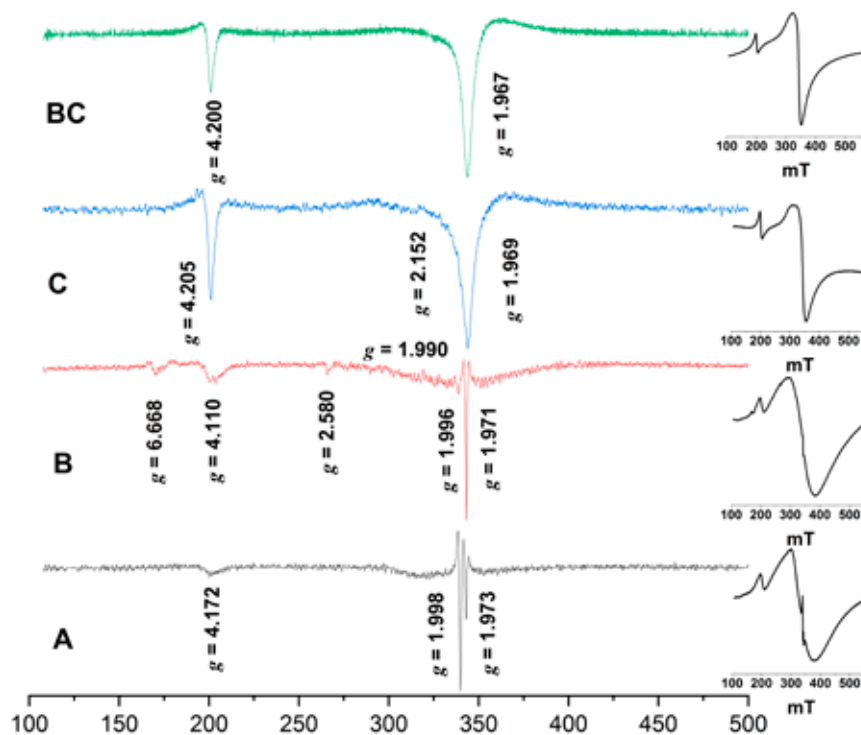

Fig. 5. EPR spectra of the samples: **A, B, C, BC** (bottom-up)

Condensed Matter and Interphases / Конденсированные среды и межфазные границы   2024;26(2): 327–338

A. G. Chetverikova et al.   The synergy of transformation of isomorphous phyllosilicate structures

3.5. Paramagnetic centers in the structure

Electron paramagnetic resonance makes it significantly easier to identify structural transformations due to the presence of paramagnetic impurities in minerals. EPR spectroscopy has recently become an important method in the studies of clays. There are a lot of studies focusing on paramagnetic centers or radicals associated with clays. The interpretation of the experimental data obtained by means of EPR spectroscopy is only possible, when reliable identification methods are used (X-ray phase analysis, IR spectroscopy).

Fe^{2+} ($3d^6$) ions are not Kramer ions and are usually invisible for EPR spectroscopy [33], while the observed Fe^{3+} ($3d^5$) ion is quite common in minerals. Fig. 5 demonstrates the second derivatives of the EPR spectra of the four samples with well identifiable signals. The frames on the right hand side show the general views of the spectra (the first derivatives).

The EPR spectrum of the initial sample (A) contained 4 peaks. A narrow peak ($\Delta B \approx 16.2$ mT), located in a weak magnetic field with $g = 4.172$ is common for phyllosilicates and corresponds to the Fe^{3+} ($J = 5/2$) ion, which replaces Al^{3+} in octahedral positions with rhombic distortion [34]. A broad ($\Delta B \approx 40$ mT) line with $g = 2.111$ indicated the presence of thin films covering the iron oxides on clay particles. Furthermore, in the field near 340 mT (338.3 and 342.5) an asymmetrical double peak is observed comprised by two narrow ($\Delta B \approx 3$ mT) lines with $g = 1.998$ and $g = 1.973$ respectively. The replacement of the native cation of the crystal lattice with a cation with a greater charge (or an anion with a smaller charge) stabilized the electron paramagnetic center in the structure, whose g-factor was usually [33] below 2. Such paramagnetic centers appeared, for instance, in the case of heterovalent isomorphism. The O^- oxygen form, common in minerals, was also observed in the EPR spectra [35].

After subjection to the MW field (sample **B**) two additional signals appeared in the spectrum. A line with $g = 4.110$ corresponding to isolated Fe^{3+} ions with distorted octahedral and tetrahedral environments became complicated on the side of the weak field with a peak with $g = 6.668$. This indicated an increase in the crystallinity of phyllosilicates. A signal with $g = 2.580$ appeared, and the line with $g = 1.990$ intensified. They are associated with [36] both the formation of a metastable iron-peroxide complex and the formation of clusters of Fe^{3+} ions in iron-containing phyllosilicates. The intensity of the signals from defects decreased by 5–6 times symbatically with their concentrations. A line with $g \approx 2$ became two times broader due to an increase in the fraction of aggregative iron oxides. Such lines are usually observed in phyllosilicates, where the Fe^{3+} ion replaces the structural Mg^{2+} ion (for instance, in chlorite).

As a result of resistance heating (sample C), the amplitude increased by 3–4 times, and the width of the low field line decreased (by $\Delta B \approx 5$ mT), because the positions of isomorphous iron ions in the lattice became equivalent. The signals associated with defects disappeared, and the fraction of aggregated iron in the paramagnetic ($g = 1.969$) and ferromagnetic ($g = 2.152$) states increased. Both lines of Fe^{3+} ions in the EPR spectrum of sample BC were the narrowest and the most symmetrical as compared to the other samples. Unlike the X-ray structural analysis, which studies the whole volume of the samples, the EPR spectroscopy allowed us to register the states of rare irregular cells with foreign paramagnetic atoms. The shift of the foreign Fe^{3+} ions from the geometric centers of octahedral crystal cells towards the minima of potential energy caused by the Jahn-Teller effect decreased the potential energy of the crystal lattice [37, 38]. At the same time, some chemical bonds forming the crystal cell became stronger, while others weakened.

4. Conclusions

The combined use of the high-temperature and MW fields results in the evolution of the structure: montmorillonite microaggregates and iron containing coatings covering them, as well as the crystal cells of three-layer clay minerals are destroyed. The octahedral layers of the particles are distorted. Foreign Fe^{3+}, ions are introduced, which then participate in the crystallization of magnetite and hematite. The most obvious structural transformations include the formation of crystalline phases of iron oxides resulting from the synergistic effect of external factors.

Condensed Matter and Interphases / Конденсированные среды и межфазные границы   2024;26(2): 327–338

A. G. Chetverikova et al.   The synergy of transformation of isomorphous phyllosilicate structures

Author contributions

Chetverikova A. G. - research concept, analysis of the results, the EPR spectroscopy, text writing and editing. Makarov V. N. - analysis of the results, DTA analysis, graphs plotting, text writing and editing. Kanygina O. N. - analysis of the results, methodology development, X-ray diffractometry, text writing and editing. Seregin M. M. - analysis of the IR spectroscopy results. Yudin A. A. - chemical analysis.

Conflict of interests

The authors declare that they have no known competing financial interests or personal relationships that could have influenced the work reported in this paper.

References

1. Kolomenskiy E. N., Korolev V. A. Information entropy analysis of the structure formation in clay soils*. *Inzhenernaya geologiya [Engineering Geology]*. 1982;(5): 34–45. (in Russ.)

2. Belachew N., Bekele G. Synergy of magnetite intercalated bentonite for enhanced adsorption of congo red dye. *Silicon*. 2020;12(3): 603–612. https://doi. org/10.1007/s12633-019-00152-2

3. Zdorenko N. M., Alyabyeva T. M., Kormosh T. M. About synergism effect of complex additive of kaolin and clay suspension. *Refractories and Industrial Ceramics*. 2012;(4-5): 64–66. (in Russ., abstract in Eng.). Available at: https://elibrary.ru/pbcinp

4. Tsotetsi T. A., Mochane M. J., Motaung T. E., ... Linganiso Z. L. Synergistic effect of EG and cloisite 15A on the thermomechanical properties and thermal conductivity of EVA/PCL blend. *Materials Research*. 2017;20(1): 109–118. https://doi. org/10.1590/1980-5373-MR-2016-0277

5. Isitman N. A., Gunduz H. O., Kaynak C. Nanoclay synergy in flame retarded/glass fibre reinforced polyamide 6. *Polymer Degradation and Stability*. 2009;94(12): 2241–2250. https://doi.org/10.1016/j.polymdegradstab.2009.08.010

6. Ayres C., Lawler D. F., Kirisits M. J., Saleh N. B. Synergy between microwave radiation and silver ions or nanoparticles for inactivating *Legionella pneumophila*. *Environmental Science and Technology Letters*. 2021;8(7): 581–588. https://doi. org/10.1021/acs.estlett.1c00371

7. Chetverikova A. G., Filyak M. M., Kanygina O. N. Influence of high-frequency microwave radiation on montmorillonite structure parameters. *Ceramica*. 2019;65(376): 635–640. https://doi.org/10.1590/0366-69132019653762767

8. Yang J. N., Li Z. Y., Xu Y. X., Nie S. B., Liu Y. Effect of nickel phyllosilicate on the morphological structure, thermal properties and wear resistance of epoxy nanocomposites. *Journal of Polymer Research*. 2020;27(9): 274. https://doi.org/10.1007/s10965-020-02250-x

9. Barry K., Lecomte-Nana G. L., Seynou M., ... Peyratout C. Comparative properties of porous phyllosilicate-based ceramics shaped by freeze-tape casting. *Ceramics*. 2022;5(1): 75–96. https://doi.org/10.3390/ceramics5010007

10. Prokhina A. V., Shapovalov N. A., Latypova M. M. Modification of the surface of clay minerals with high concentrations of montmorillonite in a high-frequency electromagnetic field*. *Sovremennye naukoemkie tekhnologii [Modern high technology]*. 2011;(1): 135–136. (in Russ.). Available at: https://elibrary.ru/nbfqnl

11 Khodosova N. A., Belchinskaya L. I., Novikova L. A. Effect of different mechanisms of heating of layered aluminosilicate on sorption processes Communication 1. Effect of preliminary thermal and electromagnetic (microwave) heating of montmorillonite on sorption of water. *Sorbtsionnye i Khromatograficheskie Protsessy*. 2017;17(5): 781–791. (in Russ.). https://doi.org/10.17308/sorpchrom.2017.17/439

12. Anisina I.N., Chetverikova A.G., Kanygina O.N. Effect of the batch mixture composition on the kinetics of sintering of montmorillonite containing clays*. *Inorganic Materials: Applied Research*. 2012;(12): 48–52. (in Russ.). Available at: https://elibrary.ru/item.asp?id=19096983

13. Anisina I.N., Chetverikova A.G., Kanygina O.N. Activation aspects of siliceous ceramics synthesis from montmorillonite containing clay*. *Vestnik of the Orenburg State University*. 2012;(4(140)): 170–174. (in Russ.). Available at: https://elibrary.ru/item.asp?id=17921809

14. Kanygina O. N., Filyak M. M., Chetverikova A. G. Microwave-induced phase transformations of natural clay in air and humid media. *Inorganic Materials*. 2018;54(9): 904–909. https://doi.org/10.1134/s0020168518090042

15. Borneman-Starynkevich I. D. *Calculating mineral formulas*. Moscow, Nauka Publ.; 1964. 218 p. (In Russ.)

16. Bulakh A. G., Zolotarev A. A., Krivovichev V. G. *Structure. Isomorphism, formulas, and classification of minerals*. Saint-Petersburg: St. Petersburg State University Publ., 2014. 132 p. (In Russ.)

17. Sokolov V. N., Chernov M. S., Shlykov V. G., ... Krupskaya V. V. Mineral nanoparticles in dispersive soils*. *Journal of Surface Investigation: X-Ray, Synchrotron and Neutron Techniques*. 2008;(9): 88–92.

Condensed Matter and Interphases / Конденсированные среды и межфазные границы   2024;26(2): 327–338

A. G. Chetverikova et al.   The synergy of transformation of isomorphous phyllosilicate structures

(In Russ.). Available at: https://elibrary.ru/item.asp?id=11155131

18. Beaufort D., Rigault C., Billon S., ... Patrier P. Chlorite and chloritization processes through mixed-layer mineral series in low-temperature geological systems – a review. *Clay Minerals*. 2015;50(4): 497–523. https://doi.org/10.1180/claymin.2015.050.4.06

19. Drits V. A., Kossovskaya A. G. *Clay minerals: smectites and mixed-layer formations*. Moscow, Nauka Publ.; 1990. 214 p. (In Russ.)

20. Makarov V. N. *An energy-based approach to the description of structural transformations in iron oxides and aluminosilicates comprising natural clay minerals*[*]. Cand. Phys.-Math. Sci. diss. of: 1.3.8. Tver: 2022. (in Russ.). Available at: https://www.dissercat.com/content/opisanie-strukturnykh-prevrashchenii-v-oksidakh-zheleza-i-alyumosilikatakh-sostavlyayushchik

21. Vanetsev A. S., Tretyakov Y. D. Microwave-assisted synthesis of individual and multicomponent oxides. *Russian Chemical Reviews*. 2007;76(5): 397–413. https://doi.org/10.1070/rc2007v076n05abeh003650

22. Escalera E., Antti M. L., Odén M. Thermal treatment and phase formation in kaolinite and illite based clays from tropical regions of Bolivia. *IOP Conference Series: Materials Science and Engineering. IOP Publishing*. 2012;31(1): 012028. https://doi.org/10.1088/1757-899x/31/1/012017

23. Makarov V. N., Kanygina O. N. Model of destruction of montmorillonite crystal structure in a microwave field. *Nanosystems: Physics, Chemistry, Mathematics*. 2020;11(2): 153-160. https://doi.org/10.17586/2220-8054-2020-11-2-153-160

24. Jovanovski G., Makreski P. Minerals from macedonia. XXX. Complementary use of vibrational spectroscopy and x-ray powder diffraction for spectra-structural study of some cyclo-, phyllo- and tectosilicate minerals. A review. *Macedonian Journal of Chemistry and Chemical Engineering*. 2016;35(2): 125–155. https://doi.org/10.20450/mjcce.2016.1047

25. Tironi A., Trezza M. A., Irassar E. F., Scian A. N. Thermal treatment of kaolin: effect on the pozzolanic activity. *Procedia Materials Science*. 2012;(1): 343–350. https://doi.org/10.1016/j.mspro.2012.06.046

26. Khang V. C., Korovkin M. V., Ananyeva L. G. Identification of clay minerals in reservoir rocks by FTIR spectroscopy. *OP Conference Series: Earth and Environmental Science*. 2016;43(1): 012004. https://doi.org/10.1088/1755-1315/43/1/012004

27. Fricke H. H., Mattenklott M., Parlar H., Hartwig A. Method for the determination of quartz and cristobalite [Air Monitoring Methods, 2015]. *The MAK-Collection for Occupational Health and Safety*. 2002;1(1): 401–436. https://doi.org/10.1002/3527600418.am0sio2fste2015

28. Tyagi B., Chudasama C. D., Jasra R. V. Determination of structural modification in acid activated montmorillonite clay by FT-IR spectroscopy. *Spectrochimica Acta Part A: Molecular and Biomolecular Spectroscopy*. 2006;64(2): 273–278. https://doi.org/10.1016/j.saa.2005.07.018

29. Kloprogge J. T., Frost R. L. Infrared emission spectroscopic study of some natural and synthetic paragonites. *Applied Spectroscopy*. 1999;53(9): 1071–1077. https://doi.org/10.1366/0003702991948071

30. Chetverikova A. G., Kanygina O. N., Filiak M. M., Ogerchuk S. A. Structural and morphological peculiarities of montmorillonite treated with microwave radiation. *Physics and Chemistry of Materials Treatment*. 2019;(3): 5–12. (In Russ., abstract in Eng.). https://doi.org/10.30791/0015-3214-2019-3-5-12

31. Comodi P., Zanazzi P. F. Structural thermal behavior of paragonite and its dehydroxylate: a high-temperature single-crystal study. *Physics and Chemistry of Minerals*. 2000;27: 377–385. https://doi.org/10.1007/s002690000085

32. Kanygina O. N., Filiak M. M., Chetverikova A. G. Structural transformations in aluminum and silicon oxides in microwave fields. *Materials Science*. 2020;5: 37–42. https://doi.org/10.31044/1684-579x-2020-0-5-37-42

33. Hall P. L. The application of electron spin resonance spectroscopy to studies of clay minerals: I. Isomorphous substitutions and external surface properties. *Clay Minerals*. 1980;15(4): 321–335. https://doi.org/10.1180/claymin.1980.015.4.01

34. Sorieul S., Allard T., Morin G., ... Calas G. Native and artificial radiation-induced defects in montmorillonite. An EPR study. *Physics and Chemistry of Minerals*. 2005;32: 1–7. https://doi.org/10.1007/s00269-004-0427-6

35. Gilinskaya L. G., Grigorieva T. N., Razvorotneva L. I., Trofimova L. B. Composition and physicochemical properties of natural blue clays[*]. *Chemistry for Sustainable Development*. 2008;16(2): 147–157. (in Russ.). Available at: https://elibrary.ru/item.asp?id=11532517

36. Badmaeva S. V. *Synthesis of Al-, Al/Fe intercalated montmorillonites and analysis of their physicochemical properties*[*]. Cand. Chem. Sci. diss.: 02.00.04. Irkutsk: 2005. (in Russ.). Available at: https://www.dissercat.com/content/sintez-al-feal-interkalirovannykh-montmorillonitov-i-issledovanie-ikh-fiziko-khimicheskikh-s

37. Worasith N., Goodman B. A., Neampan J., ... Ferrage E. Characterization of modified kaolin from the Ranong deposit Thailand by XRD, XRF, SEM, FTIR and EPR techniques. *Clay Minerals*. 2011;46(4): 539–559. https://doi.org/10.1180/claymin.2011.046.4.539

38. Kuzakov A. S. *Electron paramagnetic resonance of degenerate orbitals in three-coordinate Ni(I)*

Condensed Matter and Interphases / Конденсированные среды и межфазные границы   2024;26(2): 327–338

A. G. Chetverikova et al.   The synergy of transformation of isomorphous phyllosilicate structures

*complexes**. Cand. Phys.-Math. Sci. diss. Irkutsk: 2012. (In Russ.). https://www.dissercat.com/content/elektronnyi-paramagnitnyi-rezonans-orbitalno-vyrozhdennykh-sostoyanii-v-trikoordinatsionnykh

* *Translated by author of the article*

Information about the authors

Anna G. Chetverikova, Cand. Sci. (Phys.-Math.), Associate Professor, Dean of the Physics Faculty, Orenburg State University (Orenburg, Russian Federation).

https://orcid.org/0000-0002-7045-3588
kr-727@mail.ru

Valery N. Makarov, Cand. Sci. (Phys.-Math.), Associate Professor, Department at Physics and Methods of Teaching Physics, Orenburg State University (Orenburg, Russian Federation).

https://orcid.org/0000-0001-5749-1427
makarsvet13@gmail.com

Olga N. Kanygina, Dr. Sci. (Phys.-Math.), Professor, Professor at the Department of Chemistry, Orenburg State University (Orenburg, Russian Federation).

https://orcid.org/0000-0001-6501-900X
onkan@mail.ru

Mikhail M. Seregin, Analytical Chemist, BO-ENERGO.ASTS LLC, (Moscow, Russian Federation).

https://orcid.org/0000-0002-2263-9679
Sereginmm@lumex.ru

Alexander A. Yudin, Lector at the Department of Chemistry, Orenburg State University (Orenburg, Russian Federation).

https://orcid.org/0000-0003-2424-0781
yudin-s97@yandex.ru